Ventromedial prefrontal area 14 provides opposing regulation of threat and reward-elicited responses in the common marmoset

Zuzanna M. Stawicka[a,b,1], Roohollah Massoudi[a,b,1], Nicole K. Horst[b,c], Ken Koda[a,b,2], Philip L. R. Gaskin[a,b,3], Laith Alexander[a,b,4], Andrea M. Santangelo[a,b], Lauren McIver[a,b], Gemma J. Cockcroft[a,b], Christian M. Wood[a,b,5,6], and Angela C. Roberts[a,b,5,6]

[a]Department of Physiology, Development and Neuroscience, University of Cambridge, Cambridge CB2 3DY, United Kingdom; [b]Behavioral and Clinical Neuroscience Institute, University of Cambridge, Cambridge CB2 3EB, United Kingdom; and [c]Department of Psychology, University of Cambridge, Cambridge CB2 3EB, United Kingdom

Edited by Robert Desimone, Massachusetts Institute of Technology, Cambridge, MA, and approved August 24, 2020 (received for review June 11, 2020)

The ventromedial prefrontal cortex (vmPFC) is a key brain structure implicated in mood and anxiety disorders, based primarily on evidence from correlational neuroimaging studies. Composed of a number of brain regions with distinct architecture and connectivity, dissecting its functional heterogeneity will provide key insights into the symptomatology of these disorders. Focusing on area 14, lying on the medial and orbital surfaces of the gyrus rectus, this study addresses a key question of causality. Do changes in area 14 activity induce changes in threat- and reward-elicited responses within the nonhuman primate, the common marmoset, similar to that seen in mood and anxiety disorders? Area 14 overactivation was found to induce heightened responsivity to uncertain, low-imminence threat while blunting cardiovascular and behavioral anticipatory arousal to high-value food reward. Conversely, inactivation enhanced the arousal to high-value reward cues while dampening the acquisition of cardiovascular and behavioral responses to a Pavlovian threat cue. Basal cardiovascular activity, including heart rate variability and sympathovagal balance, which are dysfunctional in mood and anxiety disorders, are insensitive to alterations in area 14 activity as is the extinction of conditioned threat responses. The distinct pattern of dysregulation compared to neighboring region area 25 highlights the heterogeneity of function within vmPFC and reveals how the effects of area 14 overactivation on positive and negative reactivity mirror symptoms of anhedonia and anxiety that are so often comorbid in mood disorders.

ventromedial | orbitofrontal | anxiety | anhedonia | area 14

Dysfunction in ventromedial prefrontal cortex (vmPFC) is implicated in mood and anxiety disorders (1, 2). This is theorized to result from its proposed role in reward valuation and reward-guided decision making as well as threat regulation and negative emotion (refs. 1 and 3; for reviews, see refs. 4 and 5). However, there is considerable anatomical heterogeneity within the vmPFC, which likely reflects functional heterogeneity (for reviews, see refs. 1 and 6) and may well contribute to the marked individual differences in symptomatology associated with these disorders. The vmPFC variably includes subcallosal cingulate cortex extending anteriorly to the frontal pole to include medial PFC and is composed of a number of discrete cytoarchitectonically defined brain regions including areas 25, 32, 24, 14, and 10 based on the maps of Petrides (7) and Barbas (8) (Fig. 1*A*). Unfortunately, the relatively low resolution of neuroimaging and focal lesion studies in humans have failed so far to resolve this heterogeneity (but see refs. 1 and 5), although there are a few instances of differentiation in the neuroimaging literature (9, 10). Moreover, how such heterogeneity may contribute to the varied symptomatology observed in psychiatric disorders is unknown.

Although experimental studies in animals have the potential to address these issues by providing high-resolution targeting of specific regions within vmPFC and addressing direct causality, so far, this potential has not been realized. The majority of studies have taken place in rodents, but the effectiveness of translation of their findings to humans is hampered by an insufficient understanding of cross-species anatomical homology and more importantly whether these regions share analogous functions (for reviews, see refs. 6 and 11). For example, analogous functioning has been proposed between infralimbic cortex of rodent vmPFC and a region of vmPFC in humans (12) with respect to the inhibitory regulation of conditioned threat responses. However, closer inspection of that focal area within human neuroimaging studies (13–16) reveals its location to be far more rostral than caudal subgenual cingulate area 25 (sgACC-25), the putative homologous region of rodent infralimbic cortex (17). Indeed, if anything, increased activity in sgACC-25 is associated with

Significance

Ventromedial prefrontal cortex is a large heterogenous region, which is dysfunctional in mood and anxiety disorders. Unfortunately, neuroimaging and focal lesion studies in humans have failed to resolve this heterogeneity, especially in relation to the symptom domains of enhanced negative emotion, blunted positive emotion, and autonomic dysfunction. We address this issue in marmoset monkeys, which have similar prefrontal organization to humans. By comparing inactivation and overactivation of area 14 within rostral ventromedial prefrontal cortex (vmPFC) across threatening and rewarding contexts, we reveal how area 14 overactivation heightens responsivity to distal threat and blunts appetitive arousal. Its lack of effect on basal cardiovascular reactivity and expression and extinction of certain proximal threat highlight its distinct profile of effects within the vmPFC.

Author contributions: R.M., L.A., and A.C.R. designed research; R.M., N.K.H., K.K., P.L.R.G., A.M.S., L.M., G.J.C., C.M.W., and A.C.R. performed research; Z.M.S., R.M., and C.M.W. analyzed data; and Z.M.S., C.M.W., and A.C.R. wrote the paper.

The authors declare no competing interest.

This article is a PNAS Direct Submission.

[1]Z.M.S. and R.M. contributed equally to this work.

[2]Present address: Pain and Neurology, Discovery Research Laboratory for Core Therapeutic Areas, Shionogi and Co. Ltd., Osaka 541-0045, Japan.

[3]Present address: Biological Sciences, BenevolentAI, London W1T 5HD, United Kingdom.

[4]Present address: St. Thomas' Hospital, London SE1 7EH, United Kingdom.

[5]C.M.W. and A.C.R. contributed equally to this work.

[6]To whom correspondence may be addressed. Email: cmw84@cam.ac.uk or acr4@cam.ac.uk.

This article contains supporting information online at https://www.pnas.org/lookup/suppl/doi:10.1073/pnas.2009657117/-/DCSupplemental.

First published September 21, 2020.

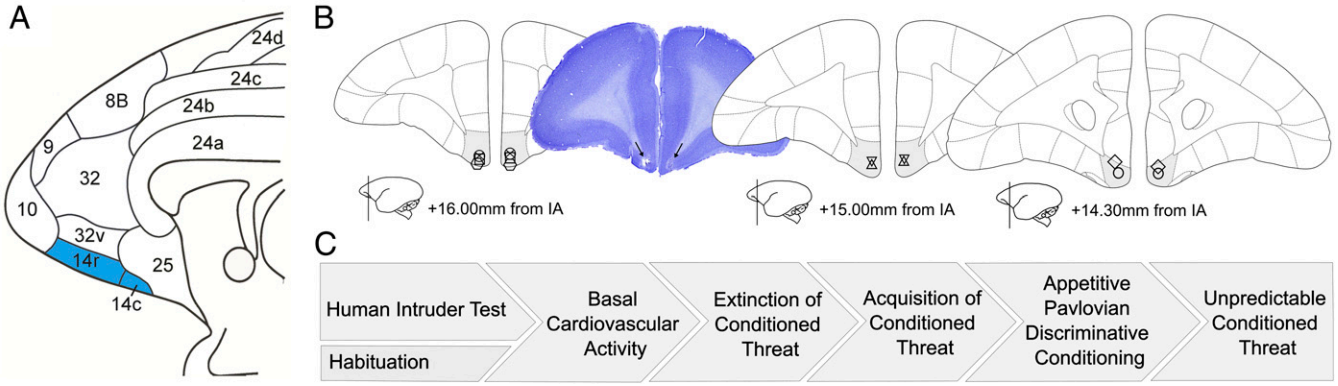

Fig. 1. Histological assessment of cannulae placements and experimental overview. (*A*) Medial view of the marmoset prefrontal and cingulate cortices, with the targeted location of area 14 highlighted in teal. This is based on the architectonic map of Paxinos et al. (78). (*B*) Schematic of coronal slices demonstrating the cannulae placement of the seven subjects in the study, with area 14 highlighted gray. The position relative to the interaural (IA) line is indicated along with a schematic showing the rostrocaudal location of the section. Individual animal's cannulae placements are indicated on the slice that lies within 0.5 mm to its location. A photomicrograph image of an example slice (subject O) stained with cresyl violet is also included with the positioning of cannulae indicated by arrows. (*C*) Flow chart demonstrating the order of experiments carried out.

treatment-resistant depression and enhanced negative emotion with successful treatment being associated with reductions of activity in this region (18).

Experimental manipulation studies in nonhuman primates are necessary to bridge this gap, in which organization of the vmPFC is far more similar to humans than that of rodents. Already, recent studies in marmosets have shown how inactivation and overactivation of caudal sgACC-25 in New World monkeys, the common marmoset (19, 20), produce effects on reward and threat-elicited responses more consistent with this region's association with enhanced negative emotion in humans than the role of the infralimbic cortex in reducing conditioned threat in rodents. However, what of the role of more rostral regions? The present study focused on area 14 in marmoset monkeys and studied its involvement in a comprehensive range of responses to both threat and reward. Area 14 was targeted since it sits anterior to sgACC-25 and is one of the areas linked to the suppression of conditioned threat in humans. Moreover, although structural and functional alterations rarely recognize anatomical boundaries, reduced activity and smaller cortical volume in a medial orbital region including area 14 is reported in patients with posttraumatic stress disorder and specific phobia (21) and cortical thickness is negatively correlated with trait anxiety [a risk factor for developing mood disorders (22)]. However, since its pattern of connections is similar to area 25, as described by Carmichael and Price (23), it might be predicted that its effects may resemble more those of area 25, and thus, like area 25, activation may be associated with enhanced negative affect. Like area 25, it has little sensory input other than that from olfactory neocortex, polymodal sensory superior temporal gyrus, and auditory input from the dorsal temporal pole but marked connectivity with limbic regions including the hypothalamus, amygdala, and periaqueductal gray as well as the hippocampus and related areas such as perirhinal and parahippocampal cortex (24). However, in comparison with area 25, the limbic connections are far less dense other than those with the hippocampus and, also unlike area 25, do not appear to include the bed nucleus of the stria terminalis (BNST) (25). Moreover, area 14 is connected to distinct circuits within the periaqueductal gray [ventrolateral periaqueductal gray (vlPAG)] compared to area 25 [dorsolateral PAG (dlPAG)] (26). Thus, differences between these two regions may be expected.

Few studies have manipulated area 14 selectively in monkeys and only one, to our knowledge, with respect to threat processing that is of relevance to our understanding of anxiety. There, monkeys were required to reach over a box containing either innately aversive stimuli, e.g., rubber snake, or neutral stimuli, in order to retrieve food reward. Excitotoxic lesions of area 14 reduced approach responses to the food reward and heightened monkeys' behavioral reactivity to both neutral and innately threatening stimuli (27). However, the specificity of these effects to threat processing are confounded by the presence of reward in this study, an issue particularly pertinent to the interpretation of the findings, since this region in monkeys has been implicated in reward comparison including the representation of reward in a common currency (28).

In the present study, therefore, we investigated selectively the contribution of area 14 to the processing of threat in a variety of different contexts in which threat is either proximal or distal, highly translatable to studies of anxiety in humans. According to the predatory imminence framework of fear and anxiety (29), negative emotions can be seen as responses along a threat continuum in time and space with different behaviors, cognitions, and emotions elicited depending upon the proximity of the threat (30), with anxiety associated with more distal threat and fear with more proximal threat. Thus, we investigated the contribution of area 14 to the regulation of responses to post-encounter distal threat (human intruder test), unpredictable proximal threat (unpredictable threat test), and predictable circa-strike threat (Pavlovian threat conditioning and extinction paradigm). Based on findings from Mobbs and colleagues (31) in humans, it is predicted that area 14 will only contribute to distal threat since prefrontal areas appear primarily activated in distal but not proximal threat conditions. In addition, we also determined the potential contribution of changes in activity in area 14 to anhedonia-like symptomatology characteristic of mood disorders. Taking into account the different underlying processes that may contribute to anhedonia in humans (32), we studied the contribution of area 14 to both anticipatory and consummatory aspects utilizing an appetitive Pavlovian conditioning paradigm. This paradigm has already successfully differentiated the different aspects of anhedonia-like behavior that can be induced by overactivation of neighboring subcallosal cingulate area 25 (20).

Given that a major characteristic of mood and anxiety disorders is alterations in cardiovascular activity, where possible we measured cardiovascular activity alongside behavior in both reward and threat paradigms. Basal cardiovascular activity was also measured independently, not only as a control for any manipulation effects on threat and reward-induced cardiovascular responses but also because it often shows dysregulation in anxiety

and mood disorders (33, 34). Since both underactivity (35–38) and overactivity (39, 40) in vmPFC have been related to mood and anxiety disorders, the effects of both inactivation (through GABA agonists) and overactivation (through glutamate reuptake inhibition) of area 14 were determined by infusions into indwelling intracerebral cannulae targeting area 14 (Fig. 1*B*; and see experimental flow chart in Fig. 1*C*). Direct comparison with findings from previous studies focused on sgACC-25 (19, 20) reveal the functional heterogeneity within vmPFC and identify the distinct function of area 14.

Results

Overactivation of Area 14 Increases Anxiety-like Behavior following Post-Encounter Distal Threat in the Form of an Unknown Human and Increases Vigilance Responses to Unpredictable Conditioned Threat. The human intruder test measures the responsivity of marmosets to a 2-min encounter with an unknown human in front of their home cage (Fig. 2*A*). It is an example of a post-encounter distal threat as described by Perusini and Fanselow (ref. 29; see review in ref. 30) since marmosets have experienced both positive and negative encounters with unknown humans and thus the current threat is uncertain. Bilateral overactivation of area 14 with dihydrokainic acid (DHK) (6.25 nmol/μL; excitatory amino acid transporter-2 inhibitor) increased anxiety-like behavior toward the human intruder compared to saline, as measured by a single latent factor (Fig. 2*B*) derived from an exploratory factor analysis of a range of behaviors displayed by a large cohort of marmosets (41). The behaviors contributing to this score include time spent at the front and back of the cage, overall height within the cage, head and body bobs, and a range of vocalizations (Fig. 2*C*). The main contributors to the anxiety-like effects of area 14 overactivation appear to be a lower time spent at the front of the cage and higher levels of head and body bobs (Table 1). Bilateral area 14 inactivation induced by muscimol-baclofen (Mus-Bac; 0.1 mM muscimol/1.0 mM baclofen) did not affect anxiety-like behaviors, with minimal change in the factor score (Table 1).

To further assess the heightened reactivity to distal threat induced by area 14 overactivation, we determined its effects in another test of unpredictable threat in a Pavlovian conditioning paradigm (Fig. 3). Here, marmosets were trained to associate an auditory cue (conditioned stimulus [CS]) with a variable presentation of innate threat (uncertain trials; 33 to 66% of trials) in the form of darkness and white noise (unconditioned threat stimulus [US+]; Fig. 3*A*). Infusions into area 14 were conducted on single test days, with sessions consisting of three trials containing a novel auditory cue (novel cue trials; 1, 2, and 5) and three of the previously trained trials containing the uncertain cue (trials 3, 4, and 6), with the US+ presented only during trial 4 (Fig. 3*B*). During novel cue trials marmosets produced a larger CS-directed vigilance response (CS period minus baseline) than during the uncertain trials, indicating an intolerance to the novel ambiguous cue (Fig. 3*C*, Saline Uncertain vs. Saline Novel). Overactivation of area 14 by DHK enhanced the vigilance response in uncertain trials, and potentiated the larger response seen in novel cue trials. DHK also increased vigilant scanning during the US, with a larger US-directed response (US period minus CS period). This hypervigilance appeared to generalize across the session with increased vigilant scanning during the baseline period before each CS period. A marked reduction in baseline heart rate (HR) accompanied the DHK-induced hypervigilant state displayed across the session.

Neither Inactivation nor Overactivation Alter Basal Cardiovascular Activity. In contrast to the above, basal cardiovascular activity in an affectively neutral context was unaffected by drug treatment in area 14 (Fig. 4), as measured by HR, as well as other indicators of autonomic control such as heart rate variability (HRV), cardiac vagal index (CVI), or cardiac sympathetic index

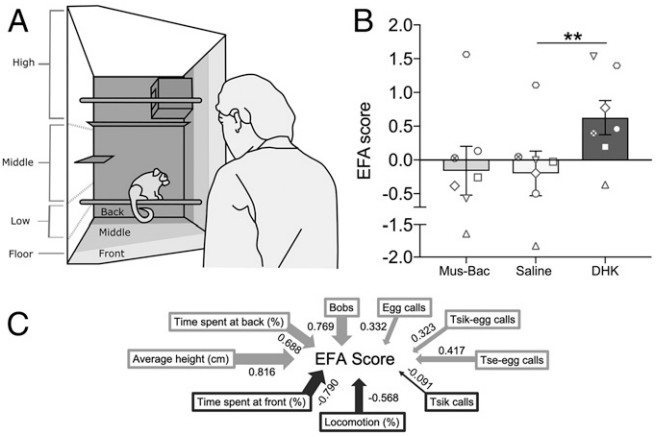

Fig. 2. Increased anxiety-like behavior in the human intruder test following overactivation of area 14. (*A*) Schematic of the testing quadrant of the home cage broken down into sectors indicating the positioning of the marmoset, e.g., front, middle, back, during a 2-min encounter with the human intruder (pictured). (*B*) Area 14 overactivation by DHK increased the exploratory factor analysis (EFA)-derived score that reflected heightened anxiety-like behaviors ($n = 7$). This was observed with a main treatment effect on EFA score [one-way ANOVA, $F_{(2,12)} = 8.58$, $P = 0.005$] with post hoc analysis showing a significant difference between DHK and saline ($P = 0.004$). No effect was observed for area 14 inactivation ($P = 0.865$). (*C*) The EFA score is generated from the range of behaviors displayed, with loadings indicated by arrow thickness; positive weighting in gray, negative weighting in black. Extensive description and evidence of the use of this EFA score to reflect anxiety-like behaviors can be found in ref. 41. Data are displayed as means with ±SEM error bars. Symbols represent individual marmosets. Significance values used are $^{**}P < 0.01$.

(CSI). While blood pressure appeared to be reduced by area 14 inactivation, this was not significant. Thus, the effect of area 14 overactivation on HR during uncertain threat appeared threat dependent. This lack of effect on basal cardiovascular activity stands in stark contrast to that seen following inactivation of the caudal vmPFC region, sgACC-25, which reduces HR and blood pressure and increases parasympathetic drive (19).

Expression and Extinction of Conditioned Threat Is Unaffected by Inactivation or Overactivation of Area 14. Since more rostral regions of vmPFC have been implicated in extinction and extinction recall of conditioned threat (13), area 14 manipulations were next studied in this context. A Pavlovian conditioned threat paradigm was presented to marmosets across a series of independent blocks. Each block was composed of five sessions: two sessions of habituation, a session of conditioning, in which a novel tone (CS) predicted the presentation of an innate threat, i.e., a rubber snake (US+), followed by a session of extinction and then extinction recall, in both of which the CS no longer predicted the snake (Fig. 5*A*). Each block was differentiated from the next by distinct patterning on the chamber walls and a novel auditory cue acting as the CS. Marmosets acquired these CS–US associations rapidly, showing marked behavioral and cardiovascular conditioning to the CS (Fig. 5 *B* and *C*, Acquisition) and sustained cardiovascular responses directed to the US (*SI Appendix*, Fig. S1), both of which did not differ across treatment blocks. A number of animals tended to show generalized increases in blood pressure across the CS and baseline period following experience with the US resulting in no overall group effect in CS-directed blood pressure (*SI Appendix*, Fig. S2); consequently, an absolute CS measure normalized to the presnake period was used.

Overactivation or inactivation of area 14 prior to extinction did not affect extinction of the conditioned cardiovascular and behavioral response when compared to saline (Fig. 5 *B* and *C*, Extinction). At the start of extinction, animals showed marked

Table 1. Effects of area 14 manipulations on the individual behaviors in the human intruder test

Measure	Contribution to EFA score	Saline	Mus-Bac	DHK	Test statistic	*P*
Time spent at front, %	−0.790	27.3 ± 12.8	32.7 ± 12.8	**14.7 ± 7.5**	3.62	**0.02***
Time spent at back, %	0.688	29.3 ± 11.3	29.8 ± 11.4	40.8 ± 7.3	1.54	0.18
Height, cm	0.816	48.7 ± 7.2	50.6 ± 5.7	56.7 ± 4.5	1.81	0.13
Head and body bobs	0.769	15.3 ± 4.9	22.3 ± 10.3	**44.5 ± 12.5**	3.26	**0.02***
Locomotion, %	−0.568	5.3 ± 1.1	4.3 ± 1.1	5.2 ± 1.7	0.07	0.95
Tsik calls	−0.091	1.2 ± 1.0	0.7 ± 0.4	1.5 ± 0.9	0.60	0.58
Tsik-egg calls	0.323	0.0 ± 0.0	0.1 ± 0.1	0.3 ± 0.3	1†	>0.999
Tse-egg calls	0.417	13.7 ± 12.5	9.6 ± 5.3	25.0 ± 9.8	13†	0.13
Egg calls	0.332	3.2 ± 1.3	5.1 ± 3.0	11.0 ± 8.5	5†	0.63
Tse calls	—	0.3 ± 0.3	0.9 ± 0.9	1.0 ± 0.7	3†	0.50
Jumps to front	—	4.3 ± 1.1	5.0 ± 1.2	5.7 ± 1.2	0.64	0.55

Analysis of individual behaviors revealed that DHK significantly decreased the time spent at the front of the cage compared to saline (post hoc *t* test with Sidak correction, $n = 7$; $P = 0.02$) while increasing the number of head and body bobs (post hoc *t* test with Sidak correction; $P = 0.02$). Level of contribution to the EFA score for individual behaviors is indicated. Test statistic column shows post hoc comparisons of saline vs. DHK using a paired *t* test T statistic. *P* values for all variables are indicated. Data are displayed as means ± SEM, where appropriate, with significance values of $*P < 0.05$.
†Wilcoxon test statistic (W) for cases of nonparametric data.

vigilant behavior and heightened blood pressure, indicating threat recall, which declined across subsequent trials in the absence of the US. There was also no effect on the recall of extinction on the following day (Fig. 5 *B* and *C*, Recall).

Acquisition of Conditioned Threat Is Impaired following Inactivation of Area 14. With minimal effects of area 14 manipulation on the extinction of conditioned proximal threat, the study then assessed whether the acquisition of these responses could be

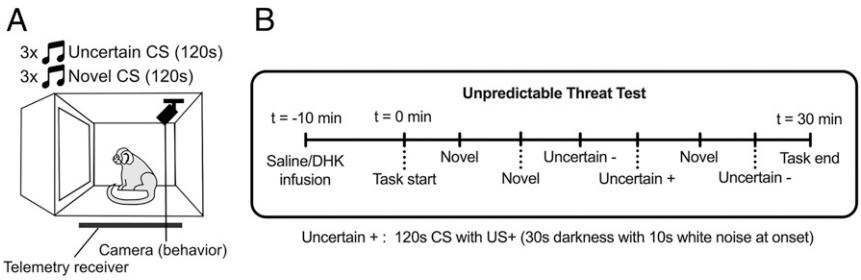

C

Variable	Uncertain trials		Novel trials	
	Saline	DHK	Saline	DHK
CS-directed				
Vigilant scanning	2.89 ± 0.90	**7.89 ± 1.69*** **	**8.83 ± 1.84##**	**16.4 ± 2.66*** ##**
Heart Rate	11.8 ± 7.52	11.6 ± 4.88	2.75 ± 3.18	0.71 ± 4.25
Baseline				
Vigilant scanning	0.39 ± 0.16	**1.78 ± 0.43****	1.17 ± 0.40	**2.94 ± 0.58***
Heart rate	283.6 ± 12.4	**264.1 ± 18.1****	289.5 ± 11.2	**270 ± 23.3***
US-directed				
Vigilant scanning	2.50 ± 0.99	**8.17 ± 0.79****		
Heart rate	10.31 ± 8.54	-4.26 ± 9.21		

Fig. 3. Overactivation of area 14 induces hypervigilant behavior to unpredictable and novel cues. (*A*) During the unpredictable threat test, marmosets were trained to associate a neutral tone with unpredictable US presentations (33 to 66% of tone trials have US per session, 8 to 12 sessions per animal; $n = 6$). Following training, marmosets were tested in single infusion sessions following area 14 manipulations (saline or DHK, at least 1 wk apart), where they received six trials, three containing the trained "uncertain" CS and three containing a novel CS for that session. Cardiovascular and behavior data were recorded throughout. (*B*) The timeline of this task and trial order on infusion sessions is indicated. (*C*) Summary table of data in the unpredictable threat test with columns separating the trial types and treatments, with rows indicating vigilant scanning and HR data during three distinct periods, CS-directed (CS period minus baseline), baseline (30 s prior to the CS onset), and US-directed (US period minus initial 30 s of CS). Focusing on vigilant scanning behavior, DHK increased CS-directed and baseline vigilant scanning for both uncertain trials and novel trials compared to saline [CS-directed: two-way ANOVA, treatment effect $F_{(1,17)} = 48.2$, $P < 0.001$; saline vs. DHK, uncertain $P < 0.001$; novel $P < 0.001$; baseline: two-way ANOVA, treatment effect $F_{(1,17)} = 18.2$, $P = 0.001$; saline vs. DHK, uncertain $P = 0.003$, novel $P = 0.017$]. The novel trials had larger CS-directed vigilant scanning responses than the uncertain trials under both DHK and saline conditions [two-way ANOVA, trial type effect $F_{(1,17)} = 19.594$, $P < 0.001$; saline, uncertain vs. novel $P = 0.0015$; DHK, uncertain vs. novel, $P = 0.0013$]. DHK also produced a larger US-directed (US minus initial 30 s of CS) vigilant scanning response compared to saline (paired *t* test, saline vs. DHK, $P = 0.008$). Focusing on HR, DHK reduced baseline HR within both trial types [two-way ANOVA, treatment effect $F_{(1,17)} = 10.81$, $P = 0.004$; saline vs. DHK, uncertain $P = 0.006$, novel $P = 0.048$]. CS-directed HR responses in novel trials were lower than uncertain trials [two-way ANOVA, trial effect $F_{(1,17)} = 6.17$, $P = 0.024$], although post hoc analyses were not significant. Data are displayed as means ± SEM, with significance values in bold illustrating Sidak-corrected pairwise comparisons following significant main effects. Treatment comparisons are indicated by asterisk (*), while trial-type comparisons indicated by number sign (#). Significance values used are $*P < 0.05$, $**P < 0.01$, and $***P < 0.001$.

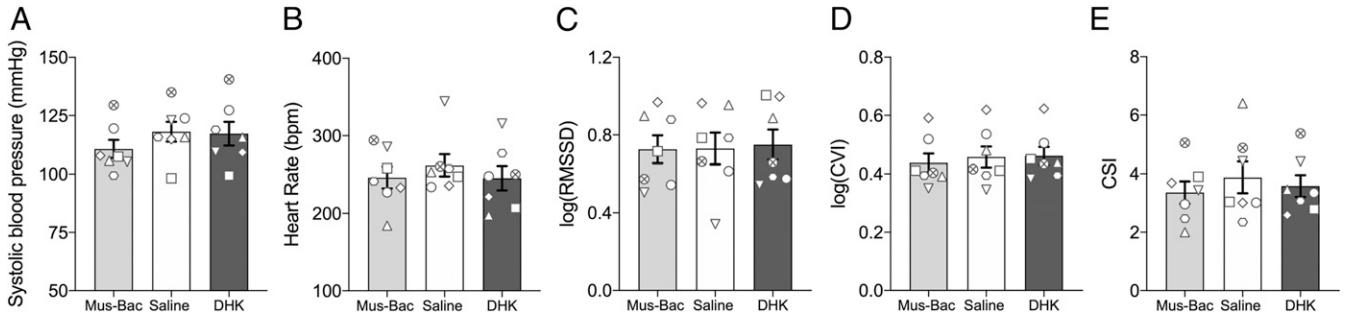

Fig. 4. Basal cardiovascular activity is insensitive to inactivation and overactivation of area 14. (*A*) In an affectively neutral environment, both inactivation (Mus-Bac) and activation (DHK) of area 14 had no effect on any cardiovascular variable ($n = 7$) when compared to saline other than a trend toward an effect on sysBP [$F_{(2,12)} = 3.48$, $P = 0.064$]. (*B–E*) No effects were observed on HR (*B*; $P = 0.486$), heart rate variability (HRV) [as measured by log-transformed root mean square of the successive differences (RMSSD)] (*C*; $F < 1$) and HRV components: cardiovagal index (*D*) [log-transformed CVI; $F_{(2,12)} = 2.77$, $P = 0.102$] and cardiosympathetic index (*E*; CSI; $F < 1$). Data are displayed as means ± SEM.

modulated by area 14 manipulation. Bilateral inactivation of area 14 by Mus-Bac (Fig. 5*D*, light gray) induced a marked impairment in both behavioral (Fig. 5*D*) and blood pressure (Fig. 5*E*) conditioning to the CS following presentation of the snake. This effect could not be explained by a lack of responsiveness to the US, since the US-induced rise in cardiovascular activity remained unaffected (Fig. 5*F*). There was no effect of area 14 overactivation.

Inactivation and Overactivation of Area 14 Produce Opposing Effects on Pavlovian Appetitive Arousal. Besides heightened responsivity to negative stimuli, a key feature of stress-related disorders is a blunting of reward processing, commonly known as anhedonia (42). Previously, we revealed that overactivation of the more caudal portion of the vmPFC, sgACC-25, induces anhedonia-like effects in the marmoset (20), so here we determined the contribution of alterations in activity of area 14 specifically in reward anticipation and consumption.

In the Pavlovian appetitive conditioning paradigm (Fig. 6*A*), animals were trained to discriminate between two CSs, one that predicted access to reward (CS+) (Fig. 6*A*, CS+ trial) and another that predicted no reward (CS−) (Fig. 6*A*, CS− trial). Successful discrimination was indicated by anticipatory increases in blood pressure and head-jerk behavior to the CS+ only. Area 14 manipulations were conducted immediately prior to a test session containing both a CS− trial and a CS+ trial, with marmosets displaying marked anticipatory cardiovascular (Fig. 6*A*) and behavioral (Fig. 6*B*) arousal to the CS+ compared to the CS− after saline infusions. Overactivation of area 14 blunted the anticipatory response to the CS+ compared to CS−, with a reduced rise in head-jerk behaviors and blood pressure (Fig. 6 *B* and *C*, DHK; for CS− and CS+ trial breakdown, see *SI Appendix*, Fig. S3). Conversely, inactivation of area 14 potentiated the anticipatory cardiovascular and behavioral arousal to the CS+ compared to CS− (Fig. 6 *B* and *C*, Mus-Bac). These effects appeared selective to anticipatory arousal as they occurred without changes to measures of US+ responsivity including amount of reward consumed (Fig. 6*D*) and rise in blood pressure (Fig. 6*E*).

Discussion

We show here that pharmacological manipulations that reduced or increased activity in area 14 produced an opposing profile of effects on threat- and reward-elicited responses. By far, the most widespread effects were seen following area 14 overactivation induced by blockade of the glutamate transporter GLT1. Anxiety-like responses to uncertain and hence more distal threat were heightened, while conditioned cardiovascular and behavioral responses to an appetitive cue were blunted. In contrast, the effects of inactivation of area 14 were more restricted. Cardiovascular and behavioral arousal to an appetitive conditioned cue was heightened, but there was no apparent effect on responsivity to distal threat or the expression or extinction of responses to proximal threat. It did, however, dampen the acquisition of conditioned behavioral and cardiovascular responses to proximal threat, while leaving sensitivity to the unconditioned threat unaffected. Although there is some overlap between the effects of area 14 manipulations with those of neighboring area 25 on threat- and reward-elicited behaviors (19, 20), there are noticeable differences, highlighting the heterogeneity of function within vmPFC in relation to its regulation of affective responses.

When considering the implications of the effects of inactivation and overactivation, it is important to recognize that only inactivation-induced changes in responsivity to reward or threat demonstrate that area 14 is necessary for the regulation of the observed reward and threat-induced responses at the time of testing. On the other hand, response effects of overactivation in the absence of effects of inactivation, only provide evidence that area 14 can contribute to these responses under certain circumstances. Importantly, in the present study, the effects of overactivation have provided direct evidence that the increased activity in vmPFC, including area 14, that has been reported in mood and anxiety disorders can contribute to threat- and reward-elicited behaviors related to specific symptoms of anxiety and anhedonia.

One major goal of this study was to test the specific hypothesis that area 14 within vmPFC contributes to the suppression of conditioned threat as suggested by correlative human neuroimaging studies. However, we observed no effects of either inactivating or activating area 14 immediately before the extinction test on either extinction of the Pavlovian conditioned cardiovascular and behavioral responses or extinction recall the next day. Thus, primate area 14 does not appear to be required for the expression of conditioned threat responses or the encoding or consolidation of extinction memory. In contrast, inactivation of area 14 did have an impact on the acquisition of conditioned threat; but, rather than the effects being consistent with a role for area 14 in suppressing conditioned threat, they instead suggested an effect on learning to acquire threat associations. Specifically, the development of both behavioral and cardiovascular conditioned responses were significantly blunted following inactivation of this region during acquisition of Pavlovian threat conditioning. The specificity of this effect was shown by the intact cardiovascular arousal induced by the innately threatening rubber snake, which acted as the US.

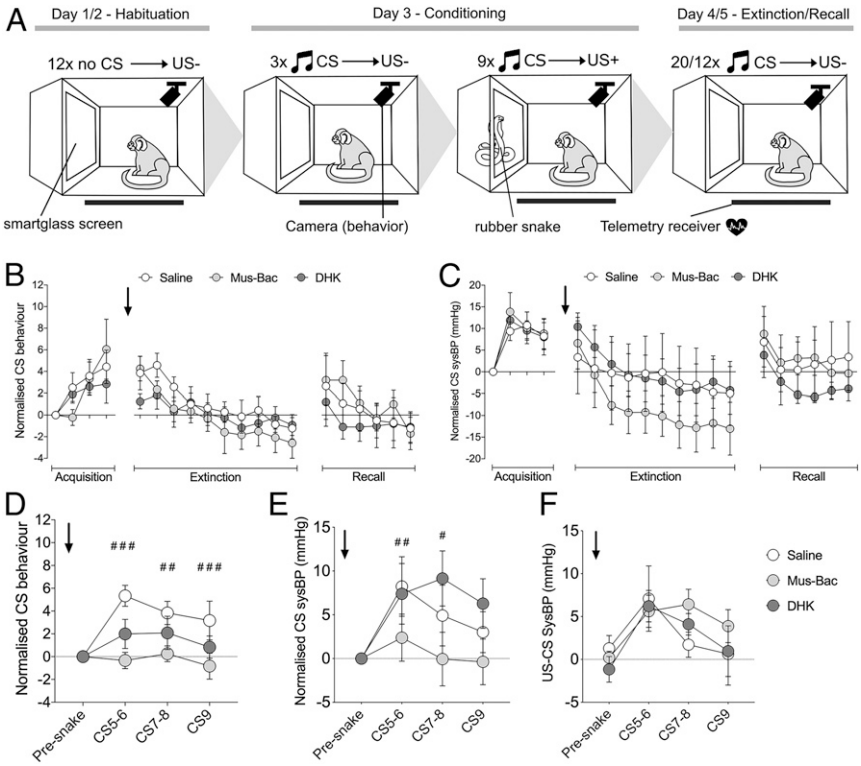

Fig. 5. Area 14 inactivation has no effect on recall or extinction of conditioned threat but blunts the acquisition of conditioned threat. (*A*) Testing on the Pavlovian conditioned threat paradigm occurred in blocks, each consisting of five daily sessions with habituation to the apparatus and smartglass (US–) on days 1/2. Animals acquired the conditioned response to the snake on day 3 as the CS predicted the rubber snake (US+). For days 4/5, the CS was presented in the absence of the US+ resulting in cardiovascular and behavioral extinction. Blocks were distinguished by distinct wall coverings and auditory CS. Drug infusions (saline, DHK, or Mus-Bac) were conducted prior to the extinction phase (graphs *B* and *C*; $n = 7$ for sysBP, $n = 6$-7 for behavior, due to loss of one video file for each MusBac and DHK groups) or acquisition phase (graphs *D*–*F*; $n = 6$) across six testing blocks. Data for graphs (*A*–*E*) were normalized to the presnake CS values, which is the first trial value. (*B*) Vigilant scanning behavior during the extinction treatment blocks. Marmosets successfully conditioned to the CS across treatment blocks during acquisition, displaying heightened vigilant scanning behavior [linear mixed effects model (CS pair × treatment); CS pair effect only, $F_{(3,58.35)} = 10.23$, $P < 0.001$]. Neither Mus-Bac or DHK influenced the rate of behavioral extinction with a decrease in vigilant scanning over the session [linear mixed effects model, CS pair effect only, $F_{(9,153.46)} = 4.26$, $P < 0.001$; treatment $F_{(2,154.44)} = 1.94$, $P = 0.34$ and CS pair x treatment F<1]. Neither manipulation affected the recall of extinction on the subsequent day (treatment and CS pair x treatment F<1). (*C*) SysBP during the extinction treatment blocks. Across all treatment blocks, marmosets successfully conditioned to the CS during acquisition, showing elevated sysBP responses [two-way ANOVA (CS pair × treatment); CS pair effect only, $F_{(3,18)} = 15.16$, $P < 0.001$], with sustained responses to the snake compared to the presnake period (*SI Appendix*, Fig. S1; two-way ANOVA [US pair × treatment block; US pair effect only, $F_{(3,18)} = 4.06$, $P = 0.023$]). Neither Mus-Bac or DHK affected the extinction of the sysBP conditioned response to the CS, with sysBP responses decreasing across the extinction session [two-way ANOVA (CS pair × treatment); CS pair effect only, $F_{(9,54)} = 15.75$, $P < 0.001$; treatment and CS pair x treatment F<1]. Neither manipulation influenced recall of this extinction on the subsequent day (Recall; treatment F<1 and CS pair x treatment, $F_{(10,60)} = 1.50$, $P = 0.17$). (*D*) Vigilant scanning behavior following drug treatment prior to acquisition. Mus-Bac blunted the acquisition of the behavioral response to the CS following introduction of the snake [two-way ANOVA (CS pair × treatment); CS × treatment interaction, $F_{(6,30)} = 3.74$, $P = 0.007$; post hoc per trial saline vs. Mus-Bac, CS5-6: $P < 0.001$; CS7-8: $P = 0.004$; CS9: $P = 0.001$]. (*E*) SysBP responses during the CS following drug manipulations prior to acquisition. Mus-Bac also reduced the sysBP responses to the CS following introduction to the snake [two-way ANOVA (CS pair × treatment); CS × treatment interaction; $F_{(6,30)} = 3.03$, $P = 0.019$; post hoc per trial, saline vs. Mus-Bac, CS5-6: $P = 0.007$; CS7-8: $P = 0.024$]. (*F*) US-directed (US minus CS) sysBP responses were unaffected by any manipulation [two-way ANOVA (US pair × treatment); US pair effect, $F_{(3,15)} = 6.06$, $P = 0.007$] with no significant treatment (F<1) or US pair by treatment effects ($F_{(6,30)} = 1.04$, $P = 0.422$). Data points display means ± SEM. Post hoc comparisons with Sidak correction significance between saline and Mus-Bac are represented as follows: $^{\#}P < 0.05$, $^{\#\#}P < 0.01$, and $^{\#\#\#}P < 0.001$.

It has been suggested that area 14, which occupies this medial orbitofrontal position in monkeys, may be functionally similar to medial orbitofrontal (MO) cortex in rats (43). However, in contrast to the effects shown here, inactivation of MO prior to extinction, using a very similar conditioning paradigm, reduced the expression of conditioned freezing (44), while effects on acquisition have not been reported. Thus, the effects seen here with respect to area 14 do not mirror effects induced by either MO or infralimbic inactivation in rats (12). They also differ markedly from the effects seen following inactivation of adjacent areas 25 and area 32 in marmosets (see Fig. 7 for anatomical maps of prefrontal and anterior cingulate cortex across species). Inactivation of both of these regions had a marked impact when induced immediately prior to extinction on the same test of Pavlovian conditioned proximal threat, with area 25 enhancing and area 32 impairing extinction (19), although neither manipulation affected subsequent recall. Thus, out of these three primate vmPFC regions, only the detrimental effects of inactivation of area 32 on threat extinction would be consistent with the proposed positive contribution of human vmPFC to the suppression of conditioned threat.

Our results differ from the heightening of defensive and avoidance responses to a rubber snake (27) seen following excitotoxic lesions of area 14 in macaques. The latter contrasts with the intact cardiovascular arousal in response to the rubber snake seen in the present study. Differences in the nature of the manipulation, namely, temporary inactivation in marmosets and permanent excitotoxic lesions in macaques could account for the

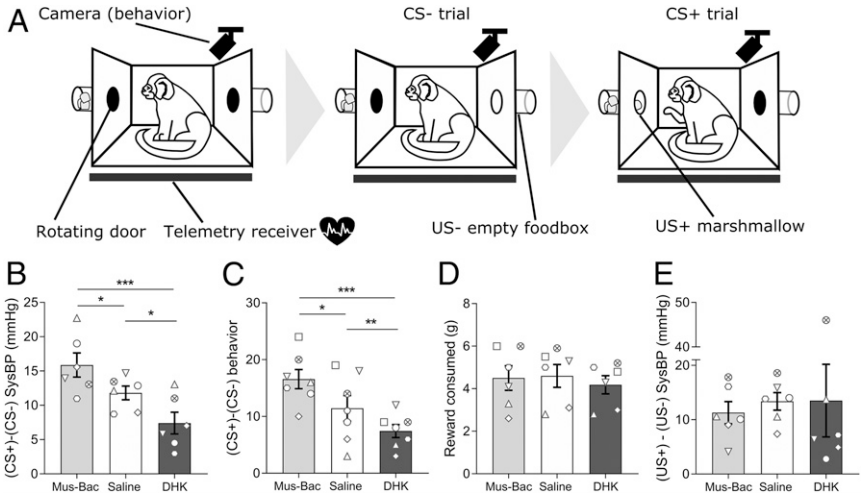

Fig. 6. Cardiovascular and behavioral arousal in anticipation of reward is enhanced and blunted by area 14 inactivation and overactivation, respectively. (*A*) In an appetitive Pavlovian discrimination task [identical to the one used previously (21)], marmosets were trained to discriminate between two auditory CSs (20 s each), one that predicted the display of an empty food box (US−, CS− trial) and one that predicted access to reward (US+, CS+ trial), with elevated blood pressure (sysBP) and head-jerk behaviors during the CS+ compared to CS− reflecting discriminative Pavlovian conditioning. Both USs were 120 s in length with the CS occurring throughout. Once stable discrimination between CSs was observed, marmosets received drug infusions prior to single sessions containing a CS− trial followed by a CS+ trial, with at least 1 wk between infusions where testing is continued to confirm the return to predrug discrimination levels. (*B*) Anticipatory arousal was blunted by DHK infusion as the CS-directed sysBP (CS-baseline) response was reduced to the CS+ compared to the CS−, while Mus-Bac produced enhanced anticipatory sysBP arousal [one-way ANOVA of difference score (CS+ minus CS−); $F_{(2,10)} = 12.68$, $P = 0.002$; post hocs, saline vs. DHK, $P = 0.026$, saline vs. Mus-Bac, $P = 0.036$]. (*C*) A similar pattern was seen for behavioral anticipatory arousal such that the enhanced arousal to the CS+ compared to the CS− was blunted by DHK infusion, and enhanced following the Mus-Bac infusion [one-way ANOVA of difference score (CS+ minus CS−); $F_{(2,12)} = 20.07$, $P < 0.001$, post hoc saline vs. DHK, $P = 0.017$, saline vs. Mus-Bac, $P = 0.04$]. Comparison of DHK and Mus-Bac responses confirm these opposing effects on both sysBP and behavior (post hoc, Mus-Bac vs. DHK, $P < 0.001$ for both). (*D*) Neither DHK nor Mus-Bac affected reward consumption. (*E*) Neither manipulation affected the sysBP arousal to the US+ compared to US−. Breakdown of CS− and CS+ trial data can be found in *SI Appendix*, Fig. S3. Data are displayed as means ± SEM ($n = 7$ for behavior, $n = 6$ for sysBP), with post hoc significance values of $*P < 0.05$, $**P < 0.01$, and $***P < 0.001$.

differences, since effects seen following permanent lesions could be the result of longer-term reorganization of networks. It is less likely to be due to differences in the extent of area 14 affected by temporary or permanent manipulations since there appeared to be no differences between animals in the current study that reflected rostrocaudal variation in cannulae placements with respect to cardiovascular responsivity to the snake (*SI Appendix*, Table S1). However, the excitotoxic lesion in macaques did encroach into neighboring regions including area 10m, which may contribute to the effect. Alternatively, differences in the nature of the cognitive processes engaged between tasks may account for differences observed given that in macaques reactivity to innate threat was measured in the context of what is effectively an approach–avoidance conflict task, whereas in marmosets, reactivity to threat was independent of reward processing. Of course, it cannot be ruled out that these regions are not functionally similar across monkey species, but this seems the least likely explanation given the comparability of the structural organization of the vmPFC across macaques and marmosets.

It is important to recognize that different networks of brain activity are engaged depending upon the proximity of the threat in time and space, and recent human neuroimaging studies suggest that prefrontal regions are primarily engaged when the threat is more distal and there is time to engage higher-order cognitive processes (31). Thus, here, we not only investigated acquisition and extinction of conditioned threat responses to proximal threat but also responsivity to post-encounter uncertain or distal threat in the form of an unknown human. Inactivation of area 14 apparently had little effect regardless of their overall level of reactivity to the human intruder. However, there was a highly pronounced increase in anxiety-like behavior following overactivation of area 14, which was mirrored by the generalization of hypervigilant scanning across the baseline of the unpredictable threat test, suggesting that under conditions of uncertainty in which area 14 is activated this can induce anxiety-like behavior.

Past studies in macaques have predominantly looked at extensive aspirative lesions of the entire orbital surface including area 14 or the more central orbital areas of 11 and 13 on the effects of responsivity to a human intruder (45–47). Here, we provide evidence for the specific effects of well-circumscribed, temporary area 14 manipulations. The anxiogenic-like effect of overactivation observed here is similar to that observed with the same treatment in neighboring sgACC-25 in marmosets (20) and is in marked contrast to the anxiogenic-like effects caused not by overactivation, but by both permanent excitotoxic lesions (48) and temporary inactivations of adjacent area 11 (49) on the orbital surface in marmosets on the same test. Overall, our findings are consistent with what is known about individual differences in structure and connectivity of area 14 in humans associated with trait anxiety (22, 50). Of particular relevance to the current results is the finding of heightened activity in the medial OFC specifically during provocation of anxiety symptoms relative to baseline in a group of patients suffering from different anxiety disorders (51). Such correlations do not indicate the direction of the relationship, but taken together with the current findings, it suggests that enhanced activity in this area may indeed heighten reactivity to an ambiguous threat.

A major characteristic of affective disorders is cardiovascular dysfunction and subsequent increases in morbidity and mortality (52, 53), and the vmPFC has been implicated as a higher-order component of the central autonomic network (54). Specifically, activity within caudal aspects of vmPFC have been shown to correlate with cardiac vagal control (34), although this did not appear to specifically encompass area 14. In the present study, only nonsignificant reductions in systolic blood pressure (sysBP) were associated with inactivation of area 14 in affectively neutral/basal conditions. This was in the absence of any changes in the

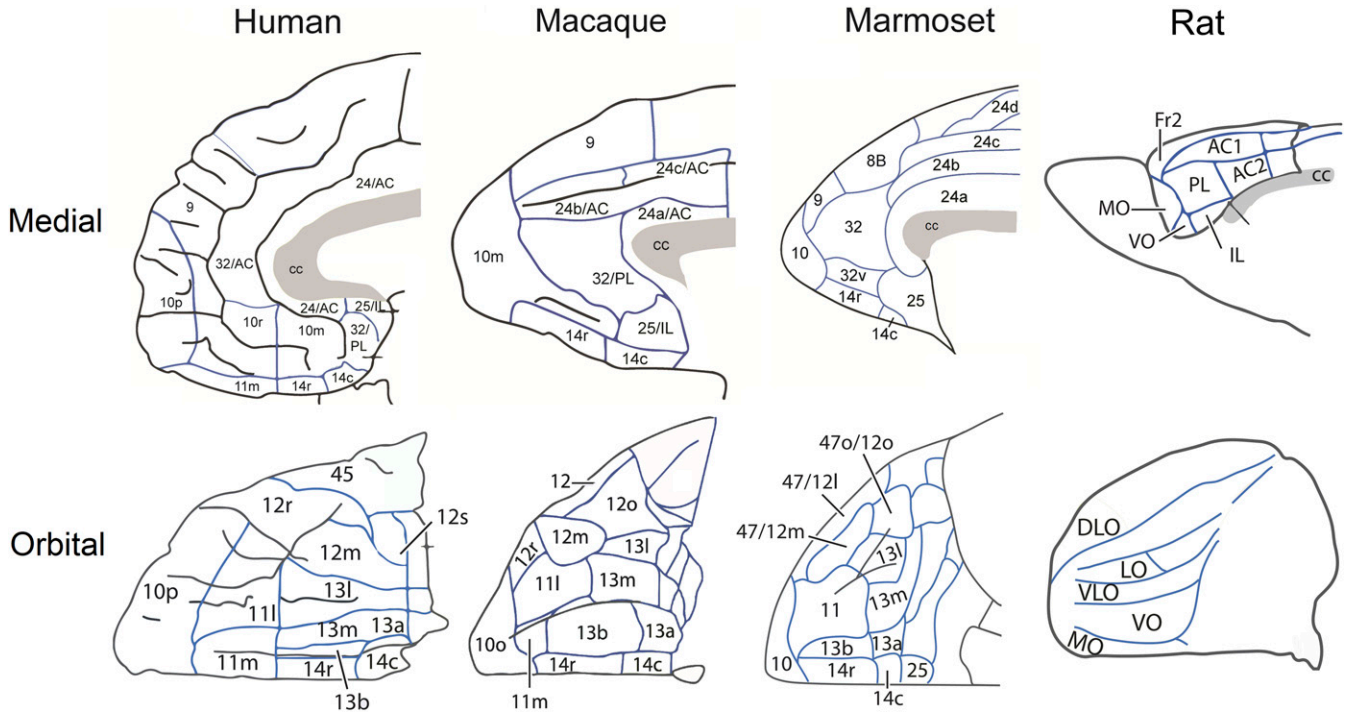

Fig. 7. Comparison of medial and orbital views of the prefrontal and cingulate cortices in humans, macaques, marmosets, and rats. Schematics of the medial and orbital views across the three species, with individual Brodmann regions identified with numbers. Parcellation maps have been labeled based on Ongür and Price (79) for the human and macaque, Paxinos et al. (78) has been used for the marmoset and Palomero-Gallagher and Zilles (80) for the rat.

CSI and CVI indices of sympathetically and vagally mediated HRV, respectively, or any effects on HR per se. Overactivation was also apparently without effect on cardiovascular activity in neutral/basal conditions. It did, however, induce a reduction in HR across the baseline in the unpredictable threat test. Since the animals showed hypervigilant scanning across the session in this test following overactivation, the reduction in HR most likely reflects a paradoxical general flattening of cardiovascular activity that has been reported to accompany high anxious states in both humans and marmosets (55, 56). Here again, the effects of area 14 manipulation are very distinct from the immediately adjacent sgACC-25, the inactivation of which had very pronounced and multiplexed effects on basal cardiovascular activity, including a reduction in HR and increased HRV driven by a shift in the balance of sympathetic to vagal-mediated control (19).

Finally, we also determined whether the effects of area 14 inactivation and overactivation extended to responsivity to cues in the reward domain. The human vmPFC, including area 14, has been implicated in the signaling of subjective reward value. Specifically, it has been suggested that area 14 is particularly involved in the direct comparison between differently valued options based on research in macaques (57–59) and humans (60, 61), and similarly medial orbitofrontal cortex in rats has been hypothesized to represent the final goal in task space (62). In the current experiment, inactivation of area 14 in the marmoset heightened the expression of both cardiovascular and behavioral discriminative conditioned responses to an appetitive cue, and conversely, overactivation blunted such responses. These effects were selective for anticipatory arousal as they occurred in the absence of any changes in cardiovascular or behavioral consummatory arousal to the food reward itself, consistent with the majority of studies of anhedonia in depression and schizophrenia in which consummatory responses appear intact (refs. 63–65, although see ref. 66 for neural changes during consummatory processing in at-risk groups). They are inconsistent, however, with a metaanalysis of imaging studies of reward processing that focused on anticipatory and outcome phases and in which activation of vmPFC regions were almost exclusively associated with the outcome phase only (67). However, close examination of the foci suggests the activations were primarily very anterior, lying within the medial frontal pole, other than those activations associated with a comparison of reward versus loss that were found more caudally, just anterior to the genu of the corpus callosum, dorsal to area 14.

Similar effects of blunting of anticipatory appetitive arousal have been reported following overactivation in sgACC-25 (20), but in the absence of effects of inactivation, we hypothesized that although sgACC-25 was not necessary for the observed anticipatory appetitive arousal responses, under circumstances in which it was activated, e.g., stress, such blunting could occur. In contrast, area 14 clearly contributes to ongoing appetitive arousal responses, and thus, if it performs an evaluative function as proposed (60, 61), the present results suggest that the loss of this function can impact even in the simple setting of a single appetitive Pavlovian cue. Why area 14's artificial activation may lead to a blunting of the anticipatory arousal response clearly needs further study, but one hypothesis may be that the animal is under the false belief that there are more valuable rewards available due to the aberrant overactivation and through a comparative mechanism reduces its response to the current reward accordingly. This would likely be through distorted activation of memory circuits as area 14 has limited sensory input (24).

In summary, area 14 had the greatest impact on the expression of anticipatory appetitive cardiovascular and behavioral arousal with inactivation enhancing, and overactivation blunting, these responses. Since overactivation has been reported within this region in depressed subjects (38), the blunting of anticipatory but not consummatory responses seen here could contribute to their anhedonia symptoms. In contrast, while inactivation had very

little effect on threat responses to proximal or distal threat, overactivation did heighten responsivity to distal and more uncertain proximal threat. This suggests that, under specific contexts, e.g., stress-induced activation, area 14 may elicit heightened reactivity to threat but only under conditions when there is time to engage additional cognitions and behaviors, consistent with the proposal from Mobbs et al. (30). These two effects of area 14 overactivation, blunting of anticipatory appetitive arousal and heightening of anxiety-like behavior, are very similar to that seen following overactivation of area 25, suggesting that these two regions likely interact in the control of the balance of reward and threat-elicited behaviors, consistent with their marked interconnectivity (23). However, area 14, unlike area 25, appears to contribute little to the regulation of basal cardiovascular activity, consistent with its relatively limited connectivity with the hypothalamus (68). Nor does it contribute to the expression or extinction of conditioned behavioral and cardiovascular arousal to certain proximal threat in stark contrast to the marked effects of both inactivation and overactivation of area 25 (19). This may reflect the far greater overall connectivity of area 25 compared to area 14 with downstream limbic structures including the amygdala (24), BNST (25), and PAG (26). Indeed, area 14 has relatively weak connectivity with the PAG and any projections are primarily targeting vlPAG linked to quiescence and passive coping. In contrast, area 25 has dense connectivity primarily with dlPAG (26), which along with lPAG is linked to initiation of active coping strategies; dlPAG is particularly associated with responsivity to psychological stressors and is distinct from physical stressors linked to the lPAG (69). Thus, area 14 provides a unique contribution to the regulation of reward and punishment-induced responses distinct from not only sgACC-25 but also neighboring areas 32 and 11 (19, 48). These findings highlight the importance of recognizing the functional fractionation of vmPFC when relating alterations in activity within this region to disorders of anxiety and depression. It also highlights the opposing effects of manipulations specifically within area 14 on reward and threat-induced responding, suggesting a role for this region in balancing the control over behavior by rewards and threats. Building on these findings, future studies should focus on how these distinct regions of vmPFC interact among themselves, as well as the prefrontal cortex as a whole, to provide global control over the regulation of reward and threat-induced responses.

Materials and Methods

Subjects and Housing. Seven experimentally naive marmosets (*Callithrix jacchus*; four males, three females) bred on site at the University of Cambridge Marmoset Breeding Colony, were housed in male–female pairs (the males were vasectomized). The room temperature was maintained at 22 ± 1 °C, with 50 ± 1% humidity, with a 12-h light–dark schedule (7 AM on; 7 PM off). The animals received a nutritionally balanced diet with water provided ad libitum. Their cages were fitted with a range of environmental enrichment. All procedures in the study were carried out in accordance with the UK Animals (Scientific Procedures) Act 1968 and University of Cambridge Animal Welfare and Ethical Review Board.

Surgical Procedures. All animals received two aseptic surgical procedures, one to implant a cardiovascular telemetric monitor into the descending aorta and another to implant intracerebral cannulae targeting area 14 bilaterally.

For all surgical procedures. Animals were premedicated with ketamine hydrochloride (0.1 mL of a 100 mg/mL solution, i.m.) and carprofen, the nonsteroidal antiinflammatory (0.03 mL of 50 mg/mL solution, s.c.). Animals were then intubated and anesthesia maintained by 2.0 to 2.5% isoflurane in 0.3 L/min oxygen. Animals were monitored with a pulse oximeter capnograph and temperature probe throughout all surgery, with temperature maintained by a heat mat. Following surgery and postoperative monitoring, marmosets received 0.1 mL (0.15 mg) of the analgesic meloxicam (Metacam) for 3 d postsurgery.

Implantation of the telemetry probe. Following intubation as described above, an incision was made down the midline of the animals' abdomen and aorta visualized. The end of the telemetry probe (HD-S10; Data Sciences International) was inserted into the descending aorta, while blood was occluded for no more than 3 min. The probe was then sutured in place within the abdomen. Animals received 0.25 mL of clavulanate-potentiated amoxicillin orally (12.5 mg, Synulox) 24 h preoperatively, 2 h, and daily for 5 d postoperatively.

Implantation of intracerebral cannulae into area 14. Following sedation and intubation as described above, animals were placed in a stereotaxic frame designed for marmosets (David Kopf). Through small holes drilled in the skull, indwelling cannulae (Plastics One) were implanted into area 14 (double stainless-steel guides, 1.4 mm apart, 7 mm in length; anteroposterior [AP], +15.5 mm; lateromedial [LM], ±0.7 mm). Coordinates were adjusted in situ based on cortical depth within the prefrontal cortex at +17.5 AP, −1.5 LM as previously reported (70), with a second adjustment within the vmPFC itself (between 8.9 and 9.3 mm) at +14.0 AP, −1.0 LM based on effective vmPFC cannulations within the laboratory (19, 20, 71). The cannulae were fixed in place with skull screws, Super Bond adhesive, and dental acrylic (Paladur). The implant was cleaned and sterile dummy cannulae and caps replaced weekly.

Intracerebral Drug Infusions. Drugs were infused under sterile conditions as previously described (71). Briefly, marmosets were gently restrained, the caps and dummy cannulae removed, and top of the cannula cleaned with a 70% isopropyl alcohol. Sterile injectors (Plastics One) connected to 10-μL Hamilton syringes in an infusion pump were then inserted, with infusions over 2 min of 0.75 μL of 0.1 mM muscimol (a $GABA_A$ agonist; Sigma-Aldrich) and 1.0 mM baclofen ($GABA_B$ agonist; Sigma-Aldrich) used for inactivation (Mus-Bac), 1 μL of DHK (glutamate transport inhibitor, 6.25 nmol/μL) for overactivation, or 1 μL of saline (control). The injector was kept in place for 1 min to allow for diffusion. Injectors were then removed, dummy cannulae and caps replaced, and animals returned to the home cage. There was a 25-min pretreatment time for Mus-Bac infusions in line with previous marmoset work (19, 71), with effects lasting 1 h in rodent studies (cited in ref. 72). There was a 10-min pretreatment time for DHK infusions, similar to that used previously (20) with maximal effects at 15 min that last for over 45 min (73). A 15-min pretreatment time for the saline control infusions was used. Drug infusion order was counterbalanced across each study. Total drug infusions per animal are indicated in *SI Appendix*, Table S1.

Behavioral Testing. All animals were tested in the same sound-attenuated apparatus for all experiments except the human intruder task, which took place in the home cage. Animals were transported to the apparatus in a clear Perspex carry box, which was placed inside and housed the marmoset throughout. The testing apparatus was fitted with a house light (3 W), speakers, a Smartglass screen (can switch between opaque and transparent—this was used for the conditioned fear task only), and three cameras (for recording behavior), with a telemetry receiver (Physiotel; Data Sciences International) hidden beneath the floor. The testing apparatus was controlled by the Whisker control system (74) and in-house software. Telemetry data were recorded throughout all sessions by Spike2 software (Cambridge Electronic Design).

Post-Encounter Distal Threat in the Form of an Unknown Human (Human Intruder Test). Testing was conducted as previously described (48) (Fig. 2*A*). This test was conducted once for each manipulation (saline, DHK, or Mus-Bac infusion). Briefly, animals were separated from their cage mate into the upper-right quadrant of their multisegment home cage following the infusion until the end of the test. Behavior was recorded using a camera (GoPro Hero 5) and microphone (Sennheiser MKE 400). For testing, animals were divided for 8 min, following which an unfamiliar human intruder entered and stood 40 cm from the cage, maintaining eye contact throughout the 2-min test. The intruder was a researcher disguised using a realistic human mask (Masks Direct) wearing familiar scrubs. Following intrusion, animals were recorded for a further 5 min. The order of masks was counterbalanced with over 1 wk between each test.

Marmosets display a range of behaviors during this test as both positive and negative experiences to novel individuals have been experienced. Behavior was scored using JWatcher software and included the position of the animal in the cage (height/depth), locomotion, and head and body bobs. Sound recordings were converted to spectrograms in Syrinx software to count the number of specific calls made including tsik, egg, tsik-egg, and tse-egg. A composite anxiety-like behavior score was derived based on the pattern of

responses using an exploratory factor analysis (EFA) of 171 marmosets response to this test, which identified a single factor that accounts for 39.7% of the total variance and has been described extensively (41). The behavioral measures associated with this factor are given different weightings based on this analysis and are located in Fig. 2*C*.

Unpredictable Conditioned Threat and Responsivity to Novel Cues. Animals were trained to associate a neutral CS with unpredictable threat over 4 d of testing, with the daily session consisting of an increasing number of trials from three to six. All trials were 2 min in length during which the CS played throughout (intertrial interval [ITI], 160 to 200 s). The threat was presented during 33 to 66% of the trials in any one session (the US; 30 s of darkness and 10 s of variably placed aversive white noise [early, middle, or late period of darkness]). Darkness onset occurred between 10 and 70 s from the CS onset. Following initial training, animals continued to be trained frequently enough to maintain the unpredictable association but not frequently enough to induce habituation to the US (two to three times weekly). The overall number of sessions prior to the first infusion was between 8 and 12 for all animals. Following stable responding, drug infusions were conducted on single testing days, with at least 1 wk between them. On infusion days, animals received the same overall session as training (six trials, 2-min length, CS throughout, ITI of 160 to 200 s) but contained three trials containing a novel CS, and three trials contained the previously experienced unpredictable CS ("uncertain CS"; Fig. 3*A*). Only one uncertain CS trial contained the US, with the US occurring 30 s from CS onset. HR and vigilant scanning behavior [an attentive visual searching behavior observed during conditioned responses to threat in marmosets (75)] were analyzed within the baseline period (BL, 30 s before CS onset), CS period (initial 30 s CS period only) for each trial as well as the US period (30 s) of trial 4. CS-directed (initial 30 s of CS period minus BL period) and US-directed (US period minus initial 30 s of CS period) scores were also calculated. HR was used within this task as it appeared to vary with task parameters better than sysBP.

Basal Cardiovascular Activity in an Affectively Neutral Context. Marmosets were habituated to the test apparatus by gradually increasing the amount of time spent inside from 5 to 15 min. The lights were kept on, and no sounds were played. Cardiovascular activity and behavior were monitored, such that once HR and sysBP were stable across the 15-min session drug infusions were conducted prior to testing in this neutral context. Animals were tested 5 d a week, with infusions at least 1 wk apart. HR, sysBP, and diastolic blood pressure were averaged across the entire session. HRV was analyzed using the root-mean-square of successive differences (RMSSD), as well as Toichi's cardiovascular sympathetic and vagal indices of HRV [CSI and CVI, respectively (76)]. These measures were calculated using interbeat interval data across the whole session using Kubios HRV software.

Conditioned Threat Acquisition and Extinction. Animals were tested on six blocks of the conditioned threat extinction paradigm [which has been described previously (19)]. Briefly, each block consisted of five testing days; two habituation sessions, acquisition (threat conditioning), extinction, and extinction recall (Fig. 5*A*). Drug infusions were conducted either prior to extinction (three extinction blocks) or acquisition (three acquisition blocks). Blocks were over 1 wk apart to minimize habituation. Blocks were distinguished by different context panels on the walls and a unique sound as the CS. Contexts and sounds were counterbalanced. For habituation, animals received 12 trials where the smartglass became transparent for 5 s revealing an illuminated empty compartment (US−; ITI, 110 to 130 s). For acquisition, animals received 12 trials during which a 25-s auditory CS (75 to 80 dB) was presented (ITI, 140 to 160 s). For the first three trials, the US− was presented during the final 5 s of each CS, while for the subsequent nine trials an innately threatening rubber snake, the US+, was displayed during the final 5 s of each CS. The rubber snake was inserted into the hidden compartment through a side hatch following the end of trial 3. The extinction session took place on the next day where animals received 20 trials containing the CS/US− pairing (ITI, 60 to 80 s). Extinction recall was conducted on the fifth day, whereby animals received 12 trials containing the CS/US− pairing (ITI, 110 to 130 s). Cardiovascular activity was measured throughout, with sysBP data extracted for the CS, US, and baseline periods (BL; 20 s prior to CS) for analysis. Behavior was quantified as the number of vigilant scanning head turns during the same periods. Of the cardiovascular measures, we focused on sysBP since HR was highly variable between and within animals and its relationship with task variables was inconsistent. Data obtained from the first and fourth trial were excluded; the former because it was the first CS exposure and often generated a surprise-like orienting response, the latter because it immediately followed introduction of the snake into the compartment, which sometimes caused a sound and a concomitant hypervigilant response. A mean was calculated for the remaining pairs of CS presentations. The data were normalized for each block by subtracting the presnake CS value from all other values for each animal, to account for individual variation.

Appetitive Discriminative Conditioning. Animals' diet on Monday to Friday was limited to pellets combined with a fruit or vegetable during this testing period. Animals were tested in the normal testing chamber with the internal apparatus modified to contain two food boxes on either side of the carry box identical to the one described by Alexander et al. (20) (Fig. 6*A*). Briefly, each food box had a rotating door, which could be open, closed, and closed but transparent. Animals were trained to associate two CSs, the CS− predicted the door becoming transparent showing an empty food box on one side and the CS+ predicted the door opening on the opposite side, giving access to marshmallow (~6 g). The protocol was run Monday to Friday, with daily testing sessions including one to two CS trials; either a single CS− or CS+, double CS−, or both CS− and CS+. Animals received five CS+ trials over 2 wk. Conditioning was assessed by examining their CS-directed arousal during the 20-s CS period relative to the immediately preceding baseline (20 s; CS-BL) for both sysBP and behavior [rapid head-jerk behavior (77)]. We focused on sysBP since HR was highly variable between and within animals in this task (20) and its relationship with task variables inconsistent. Following successful conditioning, drug infusions were carried out prior to a session containing both a CS− and CS+. Drug infusions occurred at least 1 wk apart, with nondrug test sessions throughout the week to confirm the return of normal discrimination. Difference scores were calculated for both CS-directed sysBP and behavior, by subtracting CS− responses from the CS+ (CS+ minus CS−). Blood pressure response during the US+ compared to the CS+ (US directed) and reward consumption were also calculated.

Statistical Analysis. One-way repeated-measures ANOVA with treatment as a within-subject factor was conducted for the human intruder EFA-derived score, basal cardiovascular variables, as well as appetitive discrimination data (all analyses, three levels; saline, DHK, and Mus-Bac).

Two-way repeated-measures ANOVA was conducted for the unpredictable threat test (trial type × treatment) and conditioned threat and extinction paradigm (CS pair × treatment). For conditioned threat and extinction, the analysis was conducted separately for each session (acquisition, extinction, and extinction recall). For extinction manipulations during the Conditioned Threat paradigm, behavior was analyzed using a linear mixed model analysis with Satterthwaite approximations (CS pair × treatment), due to the loss of one animal's video during acquisition. US data during the unpredictable threat test was analyzed by paired *t* test (saline vs. DHK). For all ANOVA, the Greenhouse–Geisser correction was applied if the sphericity assumption was not met. Significant effects or interactions were further analyzed using Sidak-corrected post hoc pairwise comparisons as appropriate. Nonnormal data (based on the Shapiro–Wilk test) were log transformed as appropriate, and if the transformed data were nonnormal they were analyzed using a nonparametric equivalent (Friedman test [for ANOVA] and Wilcoxon test [for paired *t* tests]).

Postmortem Assessment of Cannula Placement in Area 14. Animals were premedicated with ketamine hydrochloride (0.1 mL of a 100 mg/mL solution, i.m.) and subsequently killed with sodium pentobarbital (Dolethal; 1 mL of a 200 mg/mL solution, i.v.). Animals were then transcardially perfused with 0.1 M PBS followed by 10% formaldehyde solution. The brain was removed and placed in 10% formalin overnight, then 0.01 M PBS-azide for 48 h, and finally 30% sucrose for 72 h. The brain was sectioned using a freezing microtome (60 μm), with sections mounted onto gelatin-coated glass slides and stained with cresyl violet to confirm cannula and infusion placement within area 14 (Fig. 1*A*). All sections were visualized and photographed under a Leitz DMRD microscope.

Data Availability. Behavioral and cardiovascular data have been deposited at the Mendeley Data repository, http://dx.doi.org/10.17632/76c2j7bbbd.1 (81).

ACKNOWLEDGMENTS. We thank the University of Cambridge Biological Services staff for their care of the marmosets throughout the study. This research was funded by a Medical Research Council Programme Grant MR/M023990/1 to A.C.R. Z.M.S. was funded by a Medical Research Council Doctoral Training Programme studentship (Grant MR/N013433/1).

1. J. Hiser, M. Koenigs, The multifaceted role of the ventromedial prefrontal cortex in emotion, decision making, social cognition, and psychopathology. *Biol. Psychiatry* **83**, 638–647 (2018).
2. D. G. Andrewes, L. M. Jenkins, The role of the amygdala and the ventromedial prefrontal cortex in emotional regulation: Implications for post-traumatic stress disorder. *Neuropsychol. Rev.* **29**, 220–243 (2019).
3. P. H. Rudebeck, D. M. Bannerman, M. F. S. Rushworth, The contribution of distinct subregions of the ventromedial frontal cortex to emotion, social behavior, and decision making. *Cogn. Affect. Behav. Neurosci.* **8**, 485–497 (2008).
4. B. Myers-Schulz, M. Koenigs, Functional anatomy of ventromedial prefrontal cortex: Implications for mood and anxiety disorders. *Mol. Psychiatry* **17**, 132–141 (2012).
5. N. Palomero-Gallagher *et al*., Functional organization of human subgenual cortical areas: Relationship between architectonical segregation and connectional heterogeneity. *Neuroimage* **115**, 177–190 (2015).
6. A. C. Roberts, H. F. Clarke, Why we need nonhuman primates to study the role of ventromedial prefrontal cortex in the regulation of threat- and reward-elicited responses. *Proc. Natl. Acad. Sci. U.S.A.* **116**, 26297–26304 (2019).
7. M. Petrides, Comparative architectonic analysis of the human and the macaque frontal cortex. *Handb. Neuropsychol.* **11**, 17–58 (1994).
8. H. Barbas, D. N. Pandya, Architecture and intrinsic connections of the prefrontal cortex in the rhesus monkey. *J. Comp. Neurol.* **286**, 353–375 (1989).
9. D. V. Smith *et al*., Distinct value signals in anterior and posterior ventromedial prefrontal cortex. *J. Neurosci.* **30**, 2490–2495 (2010).
10. Z. Zhang, A. Mendelsohn, K. F. Manson, D. Schiller, I. Levy, Dissociating value representation and inhibition of inappropriate affective response during reversal learning in the ventromedial prefrontal cortex. *eNeuro* **2**, ENEURO.0072-15.2015 (2015).
11. A. C. Roberts, Prefrontal regulation of threat-elicited behaviors: A pathway to translation. *Annu. Rev. Psychol.* **71**, 357–387 (2020).
12. M. R. Milad, G. J. Quirk, Fear extinction as a model for translational neuroscience: Ten years of progress. *Annu. Rev. Psychol.* **63**, 129–151 (2012).
13. E. A. Phelps, M. R. Delgado, K. I. Nearing, J. E. LeDoux, Extinction learning in humans: Role of the amygdala and vmPFC. *Neuron* **43**, 897–905 (2004).
14. M. R. Milad *et al*., Recall of fear extinction in humans activates the ventromedial prefrontal cortex and hippocampus in concert. *Biol. Psychiatry* **62**, 446–454 (2007).
15. R. Kalisch *et al*., Context-dependent human extinction memory is mediated by a ventromedial prefrontal and hippocampal network. *J. Neurosci.* **26**, 9503–9511 (2006).
16. J. E. Dunsmoor *et al*., Role of human ventromedial prefrontal cortex in learning and recall of enhanced extinction. *J. Neurosci.* **39**, 3264–3276 (2019).
17. B. A. Vogt, G. Paxinos, Cytoarchitecture of mouse and rat cingulate cortex with human homologies. *Brain Struct. Funct.* **219**, 185–192 (2014).
18. H. S. Mayberg *et al*., "Reciprocal limbic-cortical function and negative mood: Converging PET findings in depression and normal sadness" in *Depression: The Science of Mental Health*, (Taylor and Francis, 2013), pp. 245–253.
19. C. U. Wallis, R. N. Cardinal, L. Alexander, A. C. Roberts, H. F. Clarke, Opposing roles of primate areas 25 and 32 and their putative rodent homologs in the regulation of negative emotion. *Proc. Natl. Acad. Sci. U.S.A.* **114**, E4075–E4084 (2017).
20. L. Alexander *et al*., Fractionating blunted reward processing characteristic of anhedonia by over-activating primate subgenual anterior cingulate cortex. *Neuron* **101**, 307–320.e6 (2019).
21. M. R. Milad, S. L. Rauch, The role of the orbitofrontal cortex in anxiety disorders. *Ann. N. Y. Acad. Sci.* **1121**, 546–561 (2007).
22. S. Kühn, F. Schubert, J. Gallinat, Structural correlates of trait anxiety: Reduced thickness in medial orbitofrontal cortex accompanied by volume increase in nucleus accumbens. *J. Affect. Disord.* **134**, 315–319 (2011).
23. S. T. Carmichael, J. L. Price, Connectional networks within the orbital and medial prefrontal cortex of macaque monkeys. *J. Comp. Neurol.* **371**, 179–207 (1996).
24. S. T. Carmichael, J. L. Price, Limbic connections of the orbital and medial prefrontal cortex in macaque monkeys. *J. Comp. Neurol.* **363**, 615–641 (1995).
25. S. N. Avery *et al*., BNST neurocircuitry in humans. *Neuroimage* **91**, 311–323 (2014).
26. X. An, R. Bandler, D. Ongür, J. L. Price, Prefrontal cortical projections to longitudinal columns in the midbrain periaqueductal gray in macaque monkeys. *J. Comp. Neurol.* **401**, 455–479 (1998).
27. M. S. Pujara, P. H. Rudebeck, N. K. Ciesinski, E. A. Murray, Heightened defensive responses following subtotal lesions of macaque orbitofrontal cortex. *J. Neurosci.* **39**, 4133–4141 (2019).
28. E. A. Murray, P. H. Rudebeck, Specializations for reward-guided decision-making in the primate ventral prefrontal cortex. *Nat. Rev. Neurosci.* **19**, 404–417 (2018).
29. J. N. Perusini, M. S. Fanselow, Neurobehavioral perspectives on the distinction between fear and anxiety. *Learn. Mem.* **22**, 417–425 (2015).
30. D. Mobbs, D. B. Headley, W. Ding, P. Dayan, Space, time, and fear: Survival computations along defensive circuits. *Trends Cogn. Sci.* **24**, 228–241 (2020).
31. S. Yao, S. Qi, K. M. Kendrick, D. Mobbs, Attentional set to safety recruits the ventral medial prefrontal cortex. *Sci. Rep.* **8**, 15395 (2018).
32. M. T. Treadway, D. H. Zald, Reconsidering anhedonia in depression: Lessons from translational neuroscience. *Neurosci. Biobehav. Rev.* **35**, 537–555 (2011).
33. R. M. Carney *et al*., Depression, heart rate variability, and acute myocardial infarction. *Circulation* **104**, 2024–2028 (2001).
34. R. D. Lane *et al*., Subgenual anterior cingulate cortex activity covariation with cardiac vagal control is altered in depression. *J. Affect. Disord.* **150**, 565–570 (2013).
35. P. B. Fitzgerald, A. R. Laird, J. Maller, Z. J. Daskalakis, A meta-analytic study of changes in brain activation in depression. *Hum. Brain Mapp.* **29**, 683–695 (2008).
36. H. Ito *et al*., Hypoperfusion in the limbic system and prefrontal cortex in depression: SPECT with anatomic standardization technique. *J. Nucl. Med.* **37**, 410–414 (1996).
37. H. S. Mayberg, P. J. Lewis, W. Regenold, H. N. Wagner Jr., Paralimbic hypoperfusion in unipolar depression. *J. Nucl. Med.* **35**, 929–934 (1994).
38. W. C. Drevets, J. L. Price, M. L. Furey, Brain structural and functional abnormalities in mood disorders: Implications for neurocircuitry models of depression. *Brain Struct. Funct.* **213**, 93–118 (2008).
39. W. C. Drevets *et al*., A functional anatomical study of unipolar depression. *J. Neurosci.* **12**, 3628–3641 (1992).
40. D. Ebert, K. P. Ebmeier, The role of the cingulate gyrus in depression: From functional anatomy to neurochemistry. *Biol. Psychiatry* **39**, 1044–1050 (1996).
41. S. K. L. Quah, G. J. Cockcroft, L. McIver, A. M. Santangelo, A. C. Roberts, Avoidant coping style to high imminence threat is linked to higher anxiety-like behavior. *Front. Behav. Neurosci.* **14**, 34 (2020).
42. A. Der-Avakian, A. Markou, The neurobiology of anhedonia and other reward-related deficits. *Trends Neurosci.* **35**, 68–77 (2012).
43. J. L. Price, Definition of the orbital cortex in relation to specific connections with limbic and visceral structures and other cortical regions. *Ann. N. Y. Acad. Sci.* **1121**, 54–71 (2007).
44. J. Rodriguez-Romaguera, F. H. Do-Monte, Y. Tanimura, G. J. Quirk, S. N. Haber, Enhancement of fear extinction with deep brain stimulation: Evidence for medial orbitofrontal involvement. *Neuropsychopharmacology* **40**, 1726–1733 (2015).
45. A. S. Fox *et al*., Orbitofrontal cortex lesions alter anxiety-related activity in the primate bed nucleus of stria terminalis. *J. Neurosci.* **30**, 7023–7027 (2010).
46. A. Izquierdo, R. K. Suda, E. A. Murray, Comparison of the effects of bilateral orbital prefrontal cortex lesions and amygdala lesions on emotional responses in rhesus monkeys. *J. Neurosci.* **25**, 8534–8542 (2005).
47. N. H. Kalin, S. E. Shelton, R. J. Davidson, Role of the primate orbitofrontal cortex in mediating anxious temperament. *Biol. Psychiatry* **62**, 1134–1139 (2007).
48. C. Agustín-Pavón *et al*., Lesions of ventrolateral prefrontal or anterior orbitofrontal cortex in primates heighten negative emotion. *Biol. Psychiatry* **72**, 266–272 (2012).
49. Z. M. Stawicka, R. Massoudi, L. Oikonomidis, N. K. Horst, A. C. Roberts, "Opposing contributions of subregions of the primate orbitofrontal cortex to the regulation of threat in the common marmoset" in *Neuroscience 2019 SfN Annual Meeting*, (Society for Neuroscience, 2019), p. 594.09/U38.
50. M. J. Kim, P. J. Whalen, The structural integrity of an amygdala-prefrontal pathway predicts trait anxiety. *J. Neurosci.* **29**, 11614–11618 (2009).
51. S. L. Rauch, C. R. Savage, N. M. Alpert, A. J. Fischman, M. A. Jenike, The functional neuroanatomy of anxiety: A study of three disorders using positron emission tomography and symptom provocation. *Biol. Psychiatry* **42**, 446–452 (1997).
52. N. M. Batelaan, A. Seldenrijk, M. Bot, A. J. L. M. van Balkom, B. W. J. H. Penninx, Anxiety and new onset of cardiovascular disease: Critical review and meta-analysis. *Br. J. Psychiatry* **208**, 223–231 (2016).
53. C. B. Nemeroff, P. J. Goldschmidt-Clermont, Heartache and heartbreak—the link between depression and cardiovascular disease. *Nat. Rev. Cardiol.* **9**, 526–539 (2012).
54. E. E. Benarroch, The central autonomic network: Functional organization, dysfunction, and perspective. *Mayo Clin. Proc.* **68**, 988–1001 (1993).
55. A. T. Ginty, S. M. Conklin, High perceived stress in relation to life events is associated with blunted cardiac reactivity. *Biol. Psychol.* **86**, 383–385 (2011).
56. J. L. Zeredo *et al*., Glutamate within the marmoset anterior hippocampus interacts with area 25 to regulate the behavioral and cardiovascular correlates of high-trait anxiety. *J. Neurosci.* **39**, 3094–3107 (2019).
57. M. P. Noonan *et al*., Separate value comparison and learning mechanisms in macaque medial and lateral orbitofrontal cortex. *Proc. Natl. Acad. Sci. U.S.A.* **107**, 20547–20552 (2010).
58. P. H. Rudebeck, E. A. Murray, Balkanizing the primate orbitofrontal cortex: Distinct subregions for comparing and contrasting values. *Ann. N. Y. Acad. Sci.* **1239**, 1–13 (2011).
59. G. K. Papageorgiou *et al*., Inverted activity patterns in ventromedial prefrontal cortex during value-guided decision-making in a less-is-more task. *Nat. Commun.* **8**, 1886 (2017).
60. M. P. Noonan, B. K. H. Chau, M. F. S. Rushworth, L. K. Fellows, Contrasting effects of medial and lateral orbitofrontal cortex lesions on credit assignment and decision-making in humans. *J. Neurosci.* **37**, 7023–7035 (2017).
61. T. H. B. FitzGerald, B. Seymour, R. J. Dolan, The role of human orbitofrontal cortex in value comparison for incommensurable objects. *J. Neurosci.* **29**, 8388–8395 (2009).
62. L. A. Bradfield, G. Hart, Rodent medial and lateral orbitofrontal cortices represent unique components of cognitive maps of task space. *Neurosci. Biobehav. Rev.* **108**, 287–294 (2020).
63. I. Berlin, L. Givry-Steiner, Y. Lecrubier, A. J. Puech, Measures of anhedonia and hedonic responses to sucrose in depressive and schizophrenic patients in comparison with healthy subjects. *Eur. Psychiatry* **13**, 303–309 (1998).
64. G. Arrondo *et al*., Hedonic and disgust taste perception in borderline personality disorder and depression. *Br. J. Psychiatry* **207**, 79–80 (2015).
65. G. S. Dichter, M. J. Smoski, A. B. Kampov-Polevoy, R. Gallop, J. C. Garbutt, Unipolar depression does not moderate responses to the sweet taste test. *Depress. Anxiety* **27**, 859–863 (2010).
66. C. McCabe, C. Woffindale, C. J. Harmer, P. J. Cowen, Neural processing of reward and punishment in young people at increased familial risk of depression. *Biol. Psychiatry* **72**, 588–594 (2012).
67. E. K. Diekhof, L. Kaps, P. Falkai, O. Gruber, The role of the human ventral striatum and the medial orbitofrontal cortex in the representation of reward magnitude—an activation likelihood estimation meta-analysis of neuroimaging studies of passive reward expectancy and outcome processing. *Neuropsychologia* **50**, 1252–1266 (2012).
68. D. Ongür, X. An, J. L. Price, Prefrontal cortical projections to the hypothalamus in macaque monkeys. *J. Comp. Neurol.* **401**, 480–505 (1998).

69. K. Iigaya, J. Horiuchi, L. M. McDowall, R. A. L. Dampney, Topographical specificity of regulation of respiratory and renal sympathetic activity by the midbrain dorsolateral periaqueductal gray. *Am. J. Physiol. Regul. Integr. Comp. Physiol.* **299**, R853–R861 (2010).
70. A. C. Roberts *et al*., Forebrain connectivity of the prefrontal cortex in the marmoset monkey (*Callithrix jacchus*): An anterograde and retrograde tract-tracing study. *J. Comp. Neurol.* **502**, 86–112 (2007).
71. H. F. Clarke, N. K. Horst, A. C. Roberts, Regional inactivations of primate ventral prefrontal cortex reveal two distinct mechanisms underlying negative bias in decision making. *Proc. Natl. Acad. Sci. U.S.A.* **112**, 4176–4181 (2015).
72. C. M. Stopper, S. B. Floresco, Contributions of the nucleus accumbens and its subregions to different aspects of risk-based decision making. *Cogn. Affect. Behav. Neurosci.* **11**, 97–112 (2011).
73. C. S. John *et al*., Blockade of astrocytic glutamate uptake in the prefrontal cortex induces anhedonia. *Neuropsychopharmacology* **37**, 2467–2475 (2012).
74. R. N. Cardinal, M. R. F. Aitken, Whisker: A client-server high-performance multimedia research control system. *Behav. Res. Methods* **42**, 1059–1071 (2010).
75. Y. Mikheenko *et al*., Autonomic, behavioral, and neural analyses of mild conditioned negative affect in marmosets. *Behav. Neurosci.* **124**, 192–203 (2010).
76. M. Toichi, T. Sugiura, T. Murai, A. Sengoku, A new method of assessing cardiac autonomic function and its comparison with spectral analysis and coefficient of variation of R-R interval. *J. Auton. Nerv. Syst.* **62**, 79–84 (1997).
77. Y. L. Reekie, K. Braesicke, M. S. Man, A. C. Roberts, Uncoupling of behavioral and autonomic responses after lesions of the primate orbitofrontal cortex. *Proc. Natl. Acad. Sci. U.S.A.* **105**, 9787–9792 (2008).
78. G. Paxinos, C. Watson, M. Petrides, M. Rosa, H. Tokuno, *The Marmoset Brain in Stereotaxic Coordinates*, (Elsevier, 2012).
79. D. Ongür, J. L. Price, The organization of networks within the orbital and medial prefrontal cortex of rats, monkeys and humans. *Cereb. Cortex* **10**, 206–219 (2000).
80. N. Palomero-Gallagher, K. Zilles, "Isocortex" in *The Rat Nervous System: Fourth Edition*, G. Paxinos, Ed. (Academic Press, San Diego, 2015), pp. 601–625.
81. Z. M. Stawicka *et al*, Ventromedial prefrontal area 14 provides opposing regulation of threat and reward-elicited responses in the common marmoset. *Mendeley Data* Repository. http://dx.doi.org/10.17632/76c2j7bbbd.1. Deposited 8 September 2020.